PARAMETERIZATION OF THE SURFACE-LAYER EXCHANGE COEFFICIENTS FOR ATMOSPHERIC MODELS

K. ABDELLA and N.A. McFARLANE
Canadian Centre for Climate Modelling and Analysis, Victoria, BC, Canada

(Received in final form 29 February, 1996)

Abstract. A new surface-flux parameterization is presented and its impact on climate simulations with the Canadian Centre for Climate Modelling and Analysis (CCCMA) general circulation model (GCM) is discussed. The parameterization is based on the Monin–Obukhov similarity theory using well established flux-profile relationships for the unstable conditions. However, recently proposed new relationships are used in stable conditions. The new formulation allows different roughness lengths for heat and momentum, and gives transfer coefficients that are in agreement with Monin–Obukhov similarity theory. It also includes a parameterization for the free-convective boundary layer, which often occurs over warm surfaces within light winds. In circumstances where the surface layer is not neutrally stratified the proposed flux parameterization yields surface transfer coefficients that are different from those resulting from the standard surface flux formulation used in the GCM. The most marked effects of implementing the new formulation in the GCM are found over land and adjacent oceanic regions in winter where significant differences are found in the surface heat and moisture fluxes and surface temperatures.

1. Introduction

In most modern general circulation models (GCMs) surface fluxes of heat, moisture and momentum are determined through drag and bulk transfer formulations which account for the effects of low-level wind speed and stability. Many models now have a lowest level that is close enough to the surface to permit use of Monin–Obukhov similarity theory as a framework for parameterization of surface fluxes. In these cases however it is common to use formulations that, while in qualitative agreement with surface-layer similarity theory, differ in ways that are the result of a variety of considerations including computational efficiency and attempts to account for factors such as nonhomogeneity in unresolved spatial scales.

Surface fluxes of heat and moisture play a crucial role in determining the equilibrium state of the atmosphere. Although most modern GCMs are able to reproduce the broad features of the circulation of the troposphere in a reasonably realistic manner, there is considerable variation in the fidelity with which they do so (Boer *et al.*, 1992). This is clearly so over the tropical oceans where deep convection is fueled by surface evaporation. In these circumstances the atmospheric surface layer is usually unstably stratified and it is also not uncommon for surface winds to be rather weak as well. Miller *et al.* (1992) and Godfrey *et al.* (1991) have demonstrated the marked sensitivity of simulations of major features of the tropical circulation to the parameterization of heat and moisture fluxes in these circumstances. Miller *et al.* (1992) propose a modification of the parameterization

Boundary-Layer Meteorology **80:** 223–248, 1996.

of heat and moisture fluxes in the ECMWF model in unstable conditions so as to ensure that they are not less than the free convection limit proposed by Townsend (1964).

Surface fluxes are usually relatively small when the surface layer is stably stratified. Use of the traditional log linear (Businger, 1971; Webb, 1970; Hicks, 1976) flux profile relationships in the context of Monin–Obukhov theory allows surface fluxes to vanish when some measure of stability (such as the bulk Richardson number) exceeds a finite positive value (0.2). More recent work (Beljaars and Holtslag, 1991) suggests that the log linear profiles that give rise to this feature are not valid in strongly stable conditions and, in particular, that surface fluxes may remain finite for all positive values of the bulk Richardson number.

Surface flux parameterizations in atmospheric GCMs (AGCM) typically utilize representations similar to those proposed by Louis (1979). While parameterization schemes such as these are qualitatively in agreement with Monin–Obukhov similarity theory they differ quantitatively in significant ways, an important one being that surface fluxes do typically remain non-zero for all finite values of the bulk Richardson number. As noted by Louis, this prevents decoupling of the surface from the free atmosphere in strongly stable conditions such as those which typically prevail at high latitudes in winter over continental areas and sea ice. An extension of Louis's formulation has been proposed by Garratt (1992, p. 243) and Uno *et al.* (1995). By redefining Ri_B in terms of $\Delta\theta_t = \theta_1 - \theta_t$ (where θ_t is the potential temperature at z_t which is the roughness length for heat) rather than $\Delta\theta_t = \theta_1 - \theta_s$ as in Louis's method, Uno *et al.* derive a formulation that allows momentum and heat transfer to have different roughness lengths.

As discussed by McFarlane *et al.* (1992) the surface flux parameterization used in the CCCMA GCM is similar in form (different in detail) to that of Louis (1979) in unstable conditions, and in stable conditions over land and sea ice. However it differs over open water in that surface fluxes may vanish for sufficiently large values of the bulk Richardson number. Subsequent work has led to a number of revisions of the boundary-layer treatment including development of a new surface flux parameterization scheme.

This new parameterization scheme utilizes the results of the recent work of Beljaars and Holtslag (1991) to derive a revised parameterization of surface fluxes that can be used in AGCMs. An important feature of this new parameterization is that it provides surface fluxes that are in good agreement with surface-layer similarity theory and observations over the whole range of stability conditions. In strongly stable conditions, where turbulence is intermittent, similarity theory based on the surface flux rather than the local fluxes fails. However, as discussed by Beljaars and Holtslag (1991), their proposed flux profile relationships incorporate the effects of the local fluxes, giving representation of the mean profiles well above the surface layer that agree with observation.

The purpose of the present study is to present details of the new scheme and illustrate important features of its impact on climate simulations. Although the

scheme has been designed for a newer, still developmental, version of the Canadian AGCM, its impact on climate simulations is illustrated here by presenting results for the current operational model (GCMII) as documented by McFarlane *et al.* (1992). This allows comparison with longer climate simulations made with that model using the standard surface-flux parameterization scheme.

2. Surface Flux Formulations

The surface fluxes in the atmospheric surface layer can be obtained using the similarity relations based on the Monin–Obukhov (1954) similarity theory. By using the assumption of stationary and horizontally homogeneous conditions, this theory relates the surface fluxes of momentum τ, sensible heat H and moisture Q_E to the friction velocity u_*, the temperature scale θ_* and the humidity scale q_* respectively through,

$$\begin{aligned} \tau &= \rho u_*^2 \\ H &= -\rho C_p u_* \theta_* \\ Q_E &= -\lambda \rho u_* q_* \end{aligned} \tag{1}$$

where ρ is the density of air, C_p is the specific heat at constant pressure and λ is the latent heat of vaporization. The turbulent scaling parameters can be written as a function of the mean field variables using the following integrated flux-profile relationship of Dyer (1974):

$$\begin{aligned} u_* &= \frac{kU_1}{\ln\left(\frac{z_1}{z_0}\right) - \psi_M\left(\frac{z_1}{L}\right) + \psi_M\left(\frac{z_0}{L}\right)} \\ \theta_* &= \frac{k\,\mathrm{Pr}^{-1}(\theta_1 - \theta_s)}{\ln\left(\frac{z_1}{z_t}\right) - \psi_H\left(\frac{z_1}{L}\right) + \psi_H\left(\frac{z_t}{L}\right)} \\ q_* &= \frac{k\,\mathrm{Pr}^{-1}(q_1 - q_s)}{\ln\left(\frac{z_1}{z_q}\right) - \psi_Q\left(\frac{z_1}{L}\right) + \psi_Q\left(\frac{z_q}{L}\right)}. \end{aligned} \tag{2}$$

Here k is the von Karman constant, Pr is the neutral turbulent Prandtl number, U_1 is the mean speed at height z_1, θ_s and q_s are the potential temperature and the specific humidity at the surface, z_1 is a height which is within the atmospheric surface layer, z_0, z_t and z_q are the roughness lengths for momentum, heat and moisture respectively, and L is the Obukhov length defined by

$$L = -\theta_v u_*^3 / (kg\overline{w'\theta_v'}) \tag{3}$$

where $\overline{w'\theta_v'}$ is defined to be $-u_*(\theta_* + 0.61\theta_v q_*)$, and g is the acceleration of gravity.

For Businger's (1971) form of the flux-profile relationship, Paulson (1970) and Dyer (1974) express the nondimensional stability functions $\psi_{M,H}$ as

$$\psi_M(\xi) = 2\ln(1+x) + \ln(1+x^2) - 2\tan^{-1}(x) \tag{4}$$

$$\psi_H = 2\ln(1+x^2)$$

with

$$x = (1-16\xi)^{1/4}$$

for unstable conditions ($L < 0$), while Webb (1970) proposed the log-linear relationship

$$\psi_M(\xi) = \mathrm{Pr}\,\psi_H(\xi) = -4.7\xi \tag{5}$$

for stable conditions ($L > 0$).

For the unstable surface layer the above form of the ψ functions gives very good approximations to observed flux profiles as concluded by Hogstrom (1988). However, for the stable surface-layer, Hicks (1976) and Hogstrom (1988) show that the log-linear relationship is valid only for slight stability in the range $0 < z/L < 0.5$. For stable conditions outside this range the log-linear relationship of Webb gives unrealistic surface-layer profiles. This is observed by Louis (1979) who notes that, for very stable cases, the surface becomes thermally disconnected from the atmosphere and cools the surface at a faster rate than actually observed. Holtslag (1984) concludes that this unrealistic behaviour is related to the limited range of the log-linear relationship.

More recently, in their investigation of the stable wind profile at Cabauw, Beljaars and Holtslag (1991) proposed the following, more general, form of the stability functions which do not exhibit the unrealistic behaviour that is observed with the usual log-linear relationship,

$$\begin{aligned} -\psi_M(\xi) &= a\xi + b\left(\xi - \frac{c}{d}\right)\exp(-d\xi) + \frac{bc}{d} \\ -\psi_H(\xi) &= \left(1 + \frac{2}{3}a\xi\right)^{3/2} + b\left(\xi - \frac{c}{d}\right)\exp(-d\xi) + \frac{bc}{d} - 1 \end{aligned} \tag{6}$$

where $a = 1.0$, $b = 0.667$, $c = 5$ and $d = 0.35$. By comparing the Cabauw wind data with the profiles obtained with Equation (6) Beljaars and Holtslag showed that the major part of the stable boundary layer can be well described by these forms of the stability functions.

Beljaars and Holtslag compared the momentum and heat transfer coefficients, computed by iterative solution of Equations (1)–(3) and (6) with the analytical scheme of Louis (1979) which replaces Equations (2) by

$$u_*^2 = C_{MN}F_M\left(\frac{z}{z_0}, Ri_B\right)U_1^2$$

$$u_*\theta_* = C_{HN}F_H\left(\frac{z}{z_0}, Ri_B\right)\mathrm{Pr}^{-1}U_1(\theta_1 - \theta_s) \tag{7}$$

$$u_*q_* = C_{QN}F_Q\left(\frac{z}{z_0}, Ri_B\right)\mathrm{Pr}^{-1}U_1(q_1 - q_s)$$

where C_{MN}, C_{HN} and C_{QN} are the transfer coefficients for momentum, heat and moisture in neutral conditions and F_M, F_H, and F_Q are explicit analytical functions of the bulk Richardson number

$$Ri_B = \frac{gz_1(\theta_{r1} - \theta_{rs})}{\theta_v U_1^2}. \tag{8}$$

Beljaars and Holtslag (1991) show that, for stable situations, Louis's parametrizations tend to overestimate the transfer coefficients. They also show that, for large values of the roughness length ratio z_0/z_t, Louis's formulation tends to uniform values for unstable conditions while their results actually demonstrate that the functions F_M, F_H, and F_Q dependence upon z_0/z_t can have significant influences on the sensible heat flux and the radiation budget. More recently Garratt (1992, p. 243) and Uno *et al.* (1995) developed a surface-flux formulation which takes the z_0/z_t ratio into account. Uno et al. show that the inclusion of this ratio is very important in simulating light wind and low humidity conditions.

In the CCCMA second generation general circulation model (GCMII), the transfer coefficients are computed as a function of Ri_B as:

$$(F_M, F_H) = \begin{cases} 1 + 10|Ri_B|/\left(1 + 10\left|\dfrac{Ri_B}{87A_{M,H}^2}\right|^{1/2}\right) & Ri_B < 0 \\ (1 - 5\epsilon Ri_B)^2/(1 + 10(1-\epsilon)Ri_B) & 0 \le Ri_B \le 1/5\epsilon \\ 0 & Ri_B > 1/5\epsilon \end{cases} \tag{9}$$

where

$$(A_M, A_H) = \left(\frac{z_0}{z_1}\right)^{1/2} k^2/(C_{MN}, C_{HN}). \tag{10}$$

The parameter ϵ is set to zero over land and ice-covered surfaces and to 0.3 over open water (see McFarlane *et al.*, 1992).

3. Parameterization of Transfer Coefficients

In this paper we propose analytic formulations for the heat and momentum transfer coefficients which include the effect of the ratio z_0/z_t. As pointed out by Louis

(1979) and Beljaars and Holtslag (1991) such analytic formulations are very advantageous in terms of computational efficiency since they avoid the standard iterative procedure required in order to solve the transfer equations. In our formulation we use the new stability functions of Beljaars and Holtslag for stable situations as given by Equation (6) and we use the stability functions of Dyer (1974) given by Equation (4) for unstable conditions.

Assuming that $z_q \approx z_t$ and $\psi_q \approx \psi_t$, combining Equations (2) and (3) we can write Ri_B as a function of the variable $\xi = z_1/L$,

$$Ri_B = f^{-1}\xi \tag{11}$$

where

$$f = f\left(\frac{z_1}{z_0}, \frac{z_1}{z_t}, \xi\right) = \frac{\mathrm{Pr}^{-1}\,\Psi_M^2}{\Psi_H}$$

with

$$\Psi_M = \ln\left(\frac{z_1}{z_0}\right) - \psi_M\left(\frac{z_1}{L}\right) + \psi_M\left(\frac{z_0}{L}\right) \tag{12}$$

$$\Psi_H = \ln\left(\frac{z_1}{z_t}\right) - \psi_H\left(\frac{z_1}{L}\right) + \psi_H\left(\frac{z_t}{L}\right). \tag{13}$$

As discussed by Carson and Richards (1978), Equation (11) can be numerically solved as a function of Ri_B for specified values of z_1, z_0 and z_t. Then, Equations (2) and (8) can be used to obtain the transfer coefficients.

Rather than numerically solving (11) we propose the following functions which approximately give ξ as a function of Ri_B, z_0, z_1, and z_t:

$$\xi = Ri_B A_1\left(1 + \frac{A_2}{1 - \sqrt{A_3}Ri_B}\right) \tag{14}$$

for unstable conditions and

$$\xi = Ri_B\left(\frac{A_1 + S(Ri_B)Ri_B + A_5 Ri_B^2}{A_4 Ri_B + 1}\right) \tag{15}$$

for stable conditions. Here

$$A_1 = \frac{\left(\ln\left(\frac{z_1}{z_0}\right)\right)^2}{\left(\ln\left(\frac{z_1}{z_t}\right)\right)\mathrm{Pr}}$$

$$A_2 = 1 + 5Ri_B \ln\left(\frac{z_1}{z_0}\right)\left(\frac{z_t}{z_0}\right)^{1/4}$$

$$A_3 = \frac{z_1}{\sqrt{z_0 z_t}}$$

$$A_4 = \frac{10 \ln\left(\frac{z_1}{z_0}\right)\left(1 - \frac{z_0}{z_1}\right)}{\mathrm{Pr} \ln\left(\frac{z_1}{z_0}\right)}$$

$$A_5 = \frac{27 A_4}{8 \mathrm{Pr}^2}$$

and

$$S(Ri_b) = \frac{s_1 \mathrm{Pr}\left(\ln\left(\frac{z_1}{z_t}\right)\right)^{1/2} A_5}{2 - s_2 Ri_B \exp(-s_3 Ri_B) - s_4 Ri_B^2}$$

with $s_1 = c/2 = 2.5, s_2 = (bc/d) - 1 = 8.53, s_3 = bc = 3.335$ and $s_4 = 0.05$.

These approximations, chosen to approach the asymptotic values of Equation (11) for large and small values of ξ yield transfer coefficients which are in good agreement with the iteratively solved coefficients. The function S in the stable case and the coefficient A_2 in the unstable case are included so as to account for moderate values of Ri_B and their contributions become negligible in the limit of large and small values of Ri_B.

The transfer coefficients can now be computed using the approximated ξ along with Equations (2), (4), (7) and (8) which give

$$F_M = \frac{k^2}{\Psi_M^2 C_{MN}} \tag{19a}$$

and

$$F_H = \frac{k^2}{\Psi_M \Psi_H C_{HN}} \tag{19b}$$

where Ψ_M and Ψ_H are defined by Equations (12) and (13).

4. Free-convection Conditions

Free convection occurs over warm surfaces when winds are weak. In the limit of no wind and free convection Monin–Obukhov similarity theory becomes singular. However, Beljaars (1995) showed that Monin–Obukhov theory continues to be valid provided that the near-surface wind is modified to include the free-convection velocity scale w_* given by,

$$w_* = \left(\frac{g}{T} \overline{w'\theta'_s} z_i\right)^{1/3} \tag{20}$$

where $\overline{w'\theta'_s}$ is the kinematic surface heat flux and z_i is the depth of the boundary layer. Therefore, following Beljaars (1995) we replace the mean wind U_1 in Equation (2) by the non-zero wind speed U_{1f} given by,

$$U_{1f} = (U_1^2 + (\beta w_*)^2)^{1/2} \tag{21}$$

where β is of the order of unity. This essentially redefines the bulk Richardson number Ri_B in Equation (9) in terms of U_{1f} rather than in terms of U_1. Hence, our scheme can be used as before except that the modified Richardson number must be used. In cases of moderate and strong winds this modification is negligible, while for weak winds the w_* term becomes dominant.

In order to utilize this method one has to estimate w_* which, since it depends on the surface flux, is not immediately available. In the limit of zero wind speed $U_{1f} = \beta w_*$ so that (2) gives

$$u_* = \frac{k\beta w_*}{\Psi_M} \tag{22}$$

and

$$\overline{w'\theta'_s} = \frac{k^2 \beta \omega_* \, \mathrm{Pr}^{-1}(\theta_s - \theta_1)}{\Psi_M \Psi_H}. \tag{23}$$

Substituting this into Equation (20) we obtain an approximation w_{*0}

$$w_{*0} = (b_h)^{1/3} w_b \tag{24}$$

where

$$w_b = \left(\frac{g}{T} z_i (\theta_s - \theta_1)\right)^{1/3} \tag{25}$$

and

$$b_h = \frac{k^3 \beta^{3/2} Pr^{-3/2}}{(\Psi_{M0}\Psi_{H0})^{3/2}}. \tag{26}$$

Recall that Ψ_{M0} and Ψ_{H0} as given by Equations (12) and (13) are complicated functions of L so we also need an initial approximation to L in this limit. This can be obtained by approximating Ψ_M in the definition of L to give

$$L_0 = -z_i k^3 \beta^{3/2} C_{MN}^{3/2} f_c \tag{27}$$

where we have approximated Ψ_M^{-3} by $C_{MN}^{3/2} k^{-3} f_c$ which is its neutral value multiplied by a correction function f_c given by,

$$f_c = c_1 \left(\ln\left(1 + \frac{z_0}{z_t}\right)\right)^{1/2} + c_2, \tag{28}$$

with $c_1 = 1.7$ and $c_2 = 0.9$. This factor was determined empirically and gives a good initial approximation for a wide range of momentum and heat roughness ratios and it adequately accounts for the dependence of L on the ratio z_0/z_t.

Using w_{*0} we compute a first estimate of the bulk Richardson number which will be used to obtain Ri_{B0}. This gives a first estimate to the surface flux which is used to recompute w_* using Equation (22) and a new value of Ri_B, leading to a more accurate L and hence more accurate transfer coefficients and surface fluxes. Therefore, we have the following two-step, non-iterative procedure:

1. The first estimate Ri_{B0} is calculated using w_{*0}, given by Equations (24)–(28), giving the initial estimate of the heat flux using (14), (19) and (8).
2. A second estimate, Ri_B is recalculated with a new w_* now computed from its definition as given by Equation (20). Finally L, u_*, and the final heat flux are computed using Equations (14), (19) and (8).

In principle the second step can be repeated to obtain further improvements. However, as we will see in the next section, the above two-step procedure yields results that are in excellent agreement with the fully iterated solution.

5. Numerical Examples

The transfer coefficients computed using the new approximation and the transfer coefficients computed using Equations (19) are compared with the fully iterated solution of Equation (11) in Figures 1–6. The transfer coefficients computed from the formulation of Louis *et al.* (1982) and from GCMII are also shown. In these figures the thick solid lines represent the curves computed using the full iterated solution.

For illustration, we consider conditions that correspond to various typical situations. Over the ocean, the roughness lengths are wind dependent and therefore we consider weak and strong wind conditions. Over land we consider cases with different surface roughness and different values of the ratio z_0/z_t in order to show the validity of the new formulation under the full range of conditions. We will also present results to demonstrate the accuracy of our method for free convective cases.

Figure 1 shows the transfer coefficients for heat and momentum respectively in weak wind situations over the sea. The neutral transfer coefficient for momentum, C_{MN}, that appears in the GCMII formulation as given by Equation (10) is computed using the wind dependence formulation of Smith and Banke (1975):

$$C_{MN} = 0.001R(U)$$

where

$$R(U) = \max(0.9, 0.61 + 0.063U),$$

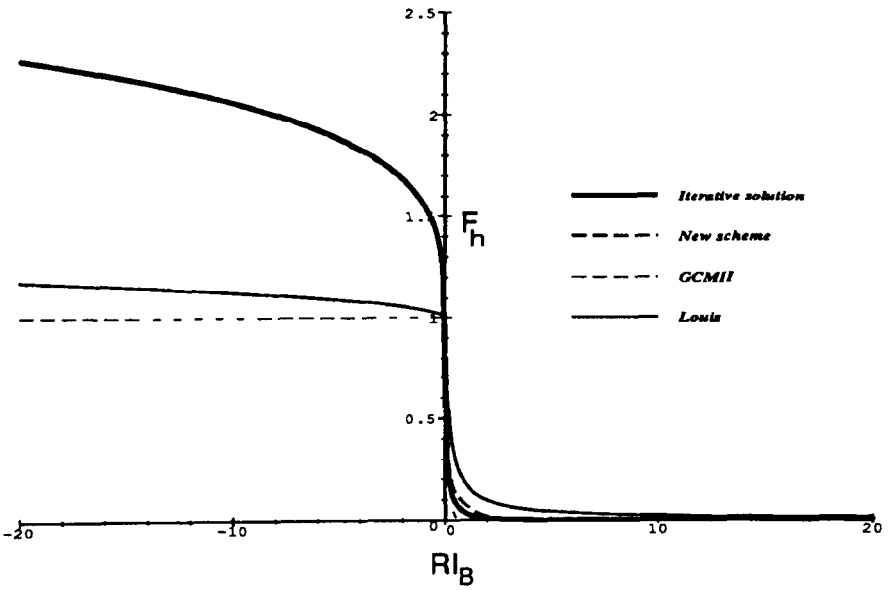

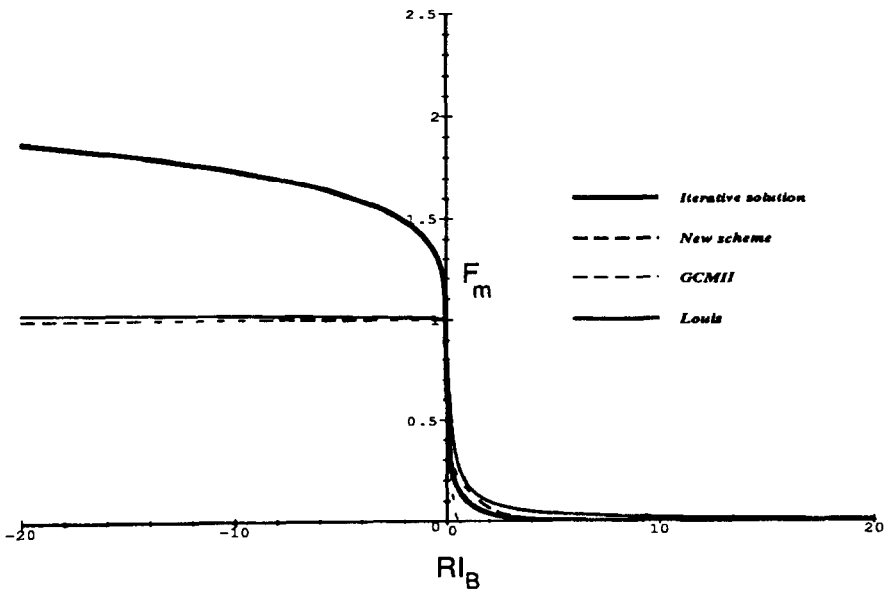

Figure 1. Heat (F_h) and momentum (F_m) transfer coefficients as a function of Ri_b for $z_0 = 1.11 \times 10^{-5}$ m, and $z_0/z_t = 0.03$.

where U is the wind speed at the 10 m shipboard anemometer level at which observational data are available. The neutral transfer coefficients for heat and moisture C_{HN} and C_{QN} (Stanton and Dalton numbers) are both assumed to be constant (C_T) with a value of 0.00115. This assumption is suggested by the work of Large and Pond (1982). However, since z_1 = 150 m in GCMII a correction factor, $S = 1 + \sqrt{C_T}\ln(z_1/10)/k$, is included in these formulations as a scaling parameter, where C_{HN} and C_{QN} are divided by S while C_{MN} is divided by S^2 and the lowest level model wind U_1 is used in computing $R(U)$ and the surface fluxes.

In GCMII, although the wind dependent C_{MN} is used in Equation (10) the roughness height z_0 that appears in that equation is assumed to be constant and is given by $z_0 = z_1 \exp^{-(k/\sqrt{C_{HN}})}$. In the comparison of the GCM simulations that will be discussed in Section 6 however, we use the more appropriate wind dependent z_0 given by $z_0 = z_1 \exp^{-(k/\sqrt{C_{MN}})}$ where the wind dependent C_{MN} is used. The roughness length for heat z_t however, is assumed to be independent of the wind speed and is computed as $z_t = z_1 \exp^{-(k/\sqrt{C_{HN}})}$. This assumption is clearly inconsistent with the wind dependent C_{MN} and a constant C_{HN}. In the next generation GCM (presently under development) these inconsistencies have been corrected by computing the 10 m wind speed from similarity theory in the Smith and Banke formulation and using the more appropriate wind dependent z_t as $z_t = z_1 \exp^{-(k\sqrt{C_{MN}}/C_{HN})}$. Results from numerical tests (not shown) suggest that even in moderately strong wind conditions, the more correct formulation gives transfer coefficients that are numerically very close to those obtained using a constant z_t in the stability functions. This is simply because strong wind conditions are usually near neutral.

For a wind speed of 2.0 m s^{-1}, it is found that $z_0 = 1.11 \times 10^{-5}$ m, $z_t = 3.46 \times 10^{-4}$ m whence $z_0/z_t = 0.03$. As shown in Figure 1, the momentum and heat transfer coefficients are highly underestimated by both Louis's formulation and the GCMII for unstable situations. In unstable conditions the transfer coefficients from the GCMII's formulation are close to unity for a broad range of Ri_B. This is due to the fact that, in this case, because z_0 is small, A_m and A_h in (10) are sufficiently small that the asymptotic correction factor $A_{m,h}|87Ri_B|^{1/2}$ is negligible for moderately large values of $-Ri_B$. Similar behaviour is observed in the curves obtained from Louis's formulation which has a similar dependence on z_0. Our new expression is in very good agreement with the fully iterated solution. In the stable conditions, the GCMII formulation has a cut off at $Ri_B = 0.66$ while the fluxes are overestimated by Louis's parameterization.

The second case, illustrated in Figure 2, represents a strong wind situation where we take the wind speed to be 15 m s^{-1}. Here we have $z_0 = 5.89 \times 10^{-4}$ m, consistent with the above remarks, z_t is unchanged ($z_t = 3.46 \times 10^{-4}$ m) and $z_0/z_t = 1.70$. The behaviour is similar to that of the weak wind situation. While excellent agreement is obtained with the new formulation, the GCMII formulation and

Louis's formulation underestimate the transfer coefficients in unstable conditions. The GCMII yields transfer coefficients that are in better agreement than the first case. The correction factor in (10) is now significant. However, in stable conditions the GCMII again gives a zero flux when Ri_B exceeds 0.66, underestimating the fluxes for highly stable conditions.

Over land there is a wide range of surface roughness. Figure 3 depicts a case over smooth surface over land with a roughness length of $z_0 = z_t = 1.15 \times 10^{-3}$ m. It is again clear from this figure that the new formulation agrees well with the fully iterated solution, whereas the GCMII and Louis's formulation both underestimate the transfer coefficients by a significant amount in the unstable case and overestimate the transfer coefficients in the stable case.

In Figure 4 we depict the heat fluxes for two cases corresponding to a rough land surface with $z_1/z_0 = 10^3$ but with different momentum to heat roughness ratio (z_0/z_t). This is important since experimental data show that a large range of this ratio has been observed. For example, for the Cabauw data, Beljaars and Holtslag (1991) find $z_0/z_t = O(10^4)$ while for the BLX83 field experiment in Oklahoma, Beljaars (1995) finds $z_0/z_t = O(10^7)$. Figure 4a and 4b depict the heat flux for the cases where $z_0/z_t = 1$ and $z_0/z_t = 10^5$ respectively. Unlike the smooth surface case GCMII tends to overestimate the heat flux in the unstable situations. This is because the transfer coefficients as they are parameterized in GCMII do not incorporate the large variation of this ratio. The new parameterization performs very well in both of these cases as compared to the fully iterated solutions. In stable conditions the result is the same as in the smooth surface case, with both GCMII and Louis's formulations overestimating the transfer coefficients.

In order to demonstrate the validity of the free convection formulation we consider a case where $z_1/z_0 = 750$ and $z_0/z_t = 10^3$ and the temperature difference $\Delta\theta = \theta_s - \theta_1 = 2$ K, and $z_i = 1000$ m. Figure 5a shows the heat flux as a function of the wind speed U_1 computed using the two-step non-iterative formulation described in the previous section with $\beta = 1.2$. It agrees well with the curve computed by iterating over the free convection velocity scale w_* with $\beta = 1.2$. As expected the curve computed using the standard Monin–Obukhov formulation (i.e. $\beta = 0$) is quite different from the $\beta = 1.2$ curves for weak winds. In weak wind conditions the w_* adjustment to the wind speed U_1 becomes important. Figure 5b shows the ratio of the modified wind speed U_{f1} and U_1 as a function of U_1. The ratio is large for weak winds but becomes unity at about $U_1 = 4.5$ m s^{-1}. A similar result is obtained for the smooth surface case as depicted in Figure 6, where $z_1/z_0 = 1.5 \times 10^6$ with all the other parameters set to be the same as in Figure 5.

Other tests carried out to investigate the sensitivities of the new formulation to the roughness-length ratios and wind conditions, including free convection cases, produce very similar results. In all the cases we took into consideration, the new formulation gives transfer coefficients which are consistent with the fully iterated solutions.

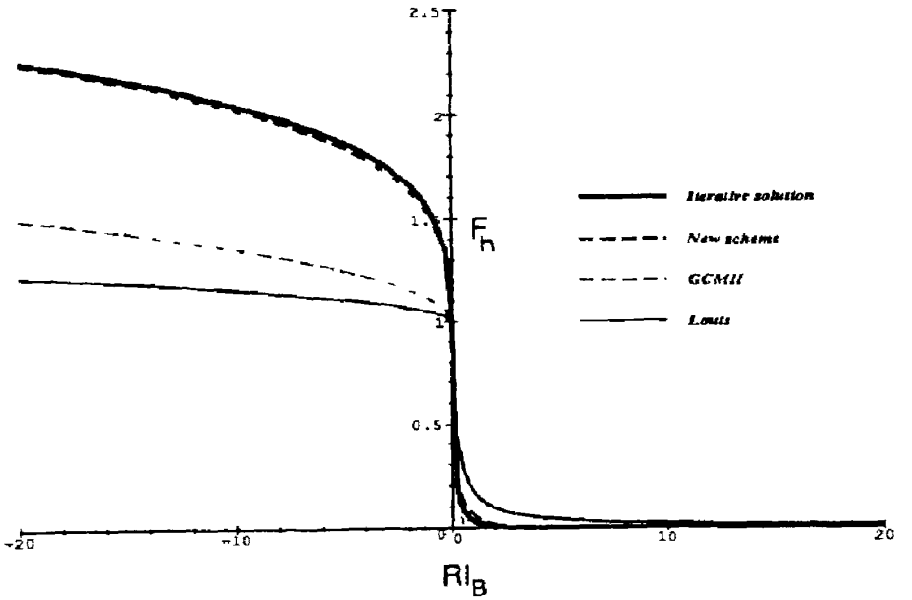

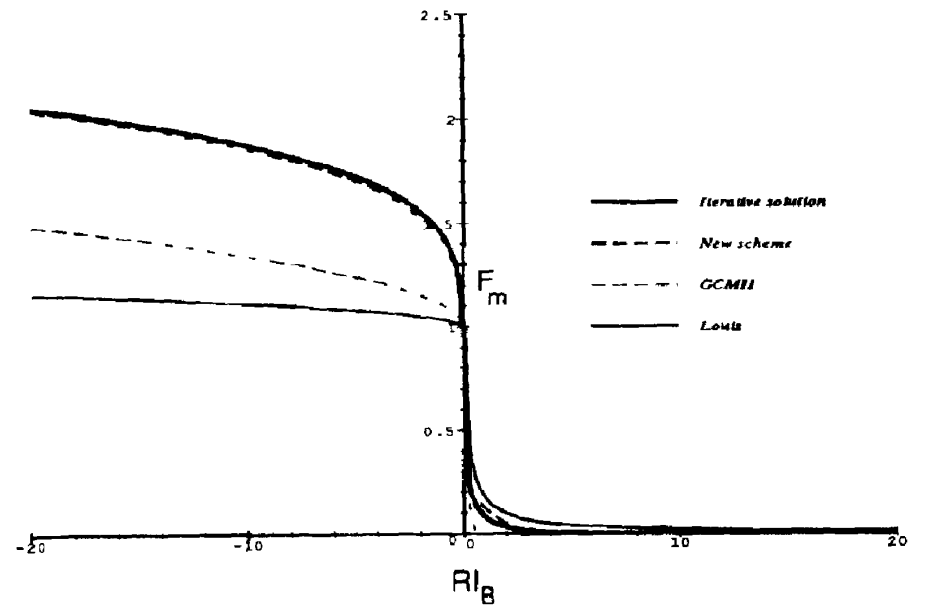

Figure 2. Heat (F_h) and momentum (F_m) transfer coefficients as a function of Ri_b for $z_0 = 5.89 \times 10^{-4}$ m, and $z_0/z_t = 1.70$.

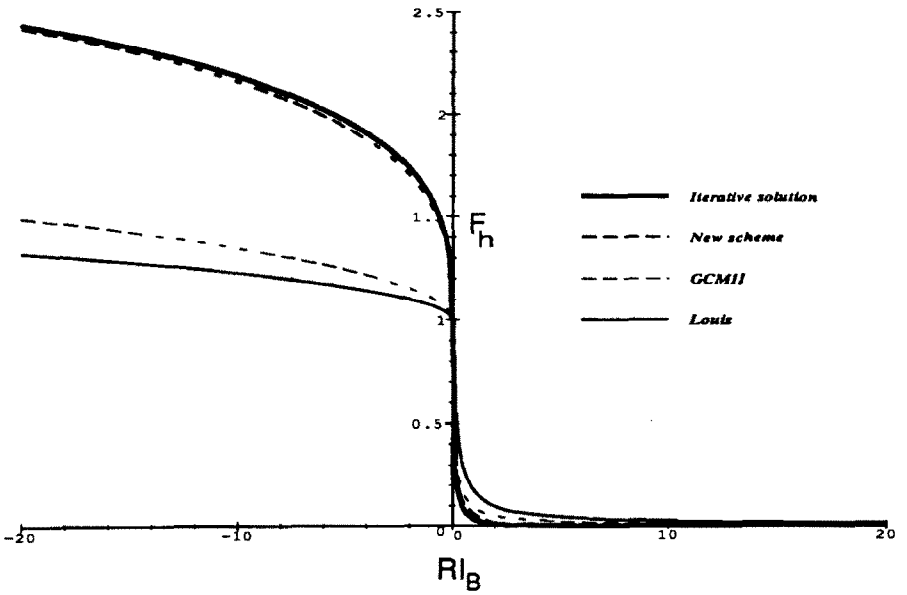

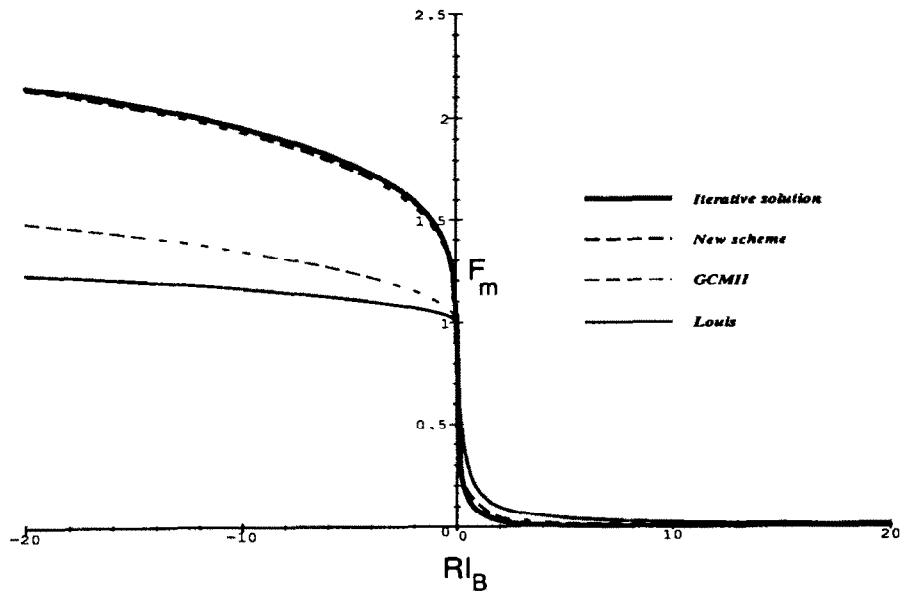

Figure 3. Heat (F_h) and momentum (F_m) transfer coefficients as a function of Ri_b for $z_0 = 1.15 \times 10^{-3}$ m, and $z_0/z_t = 1.0$.

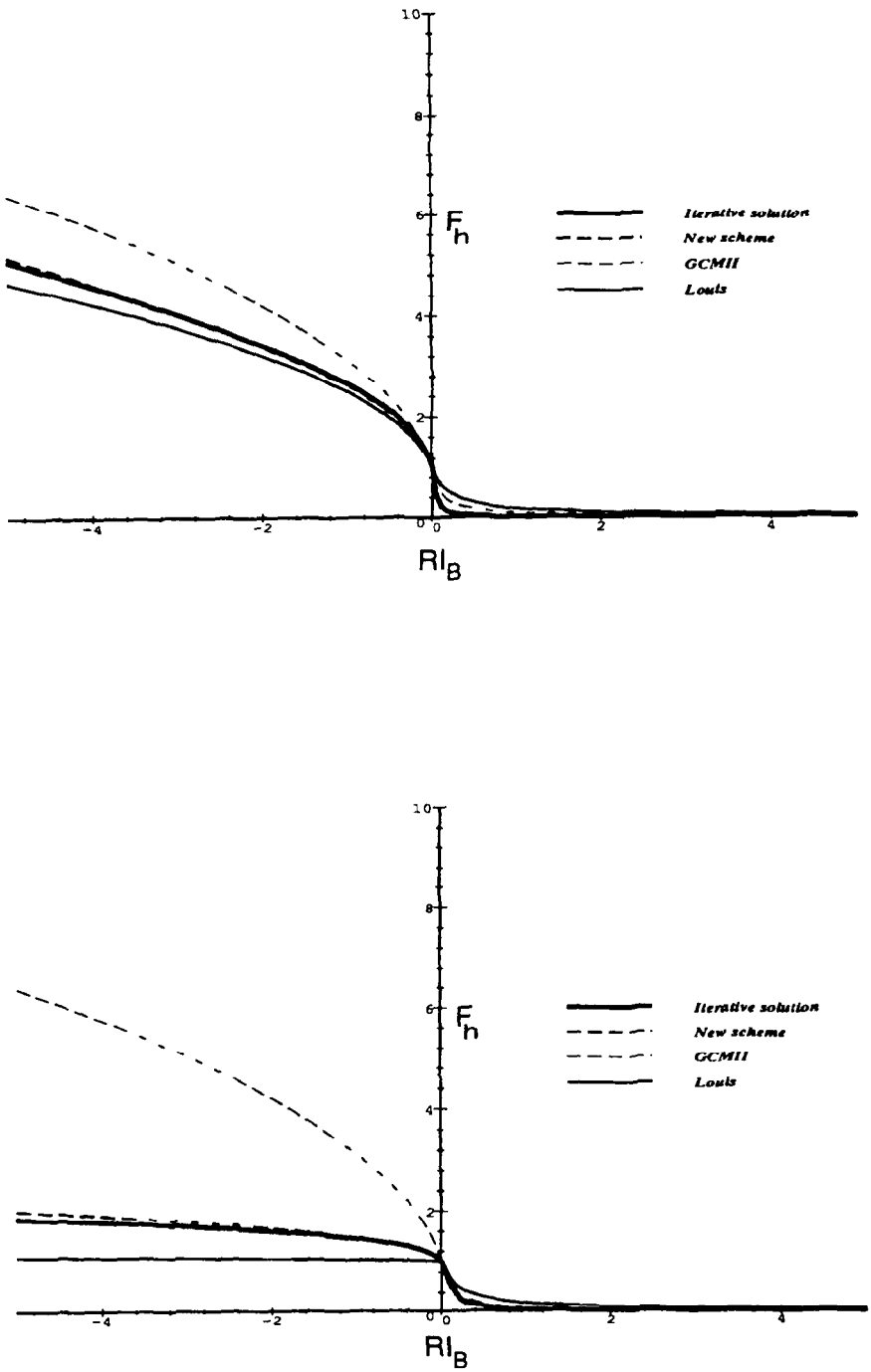

Figure 4. Heat transfer coefficients as a function of Ri_b for $z_1/z_0 = 10^3$ and $z_0/z_t = 1$ (upper), $z_0/z_t = 10^5$ (lower).

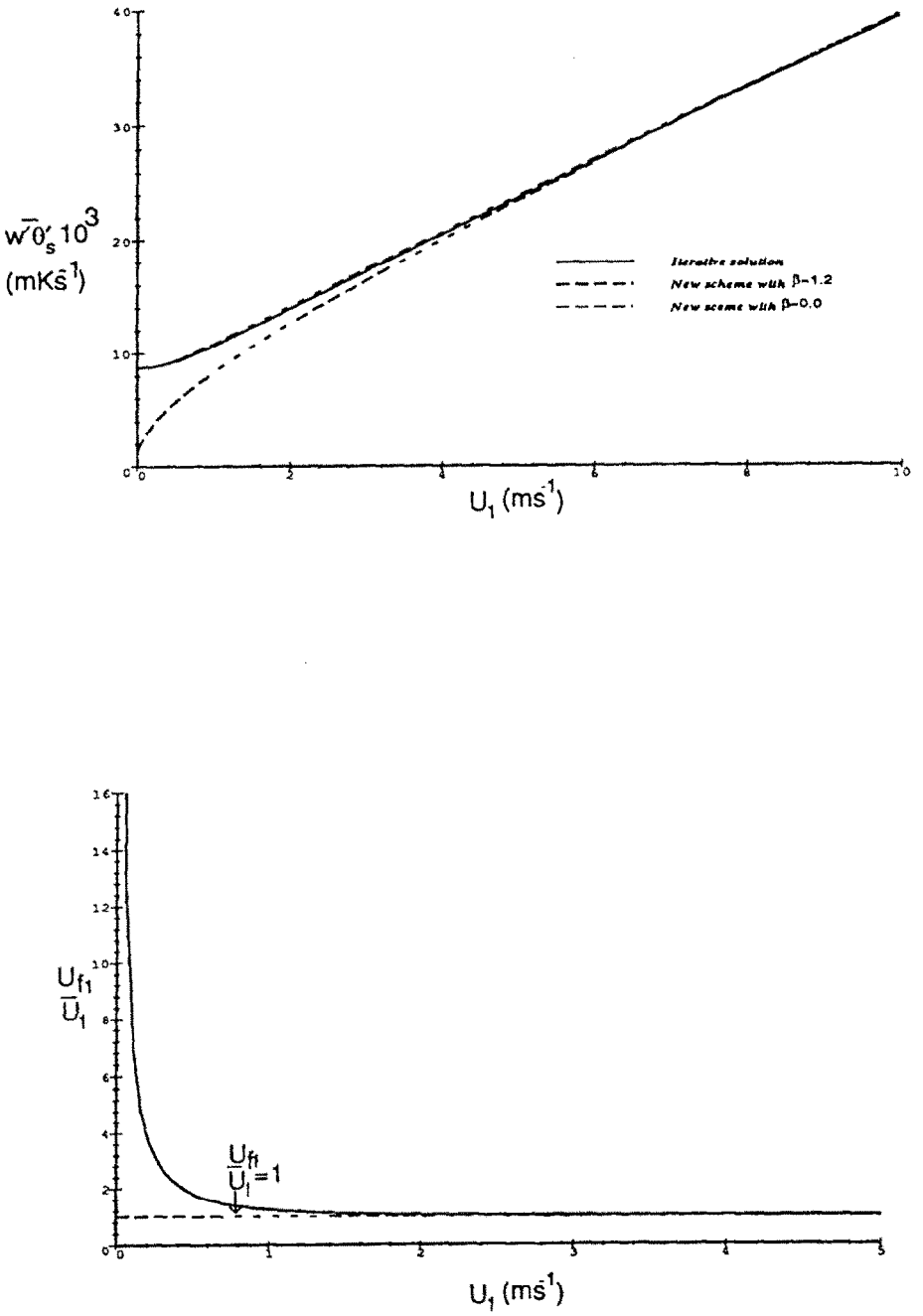

Figure 5. Upper: The heat flux as a function of U_1; lower: U_{f1}/U_1 as a function of the wind speed for the case where $z_1/z_0 = 750$, $z_0/z_t = 10^3$, $\Delta\theta = 2K$, and $z_i = 1000$ m.

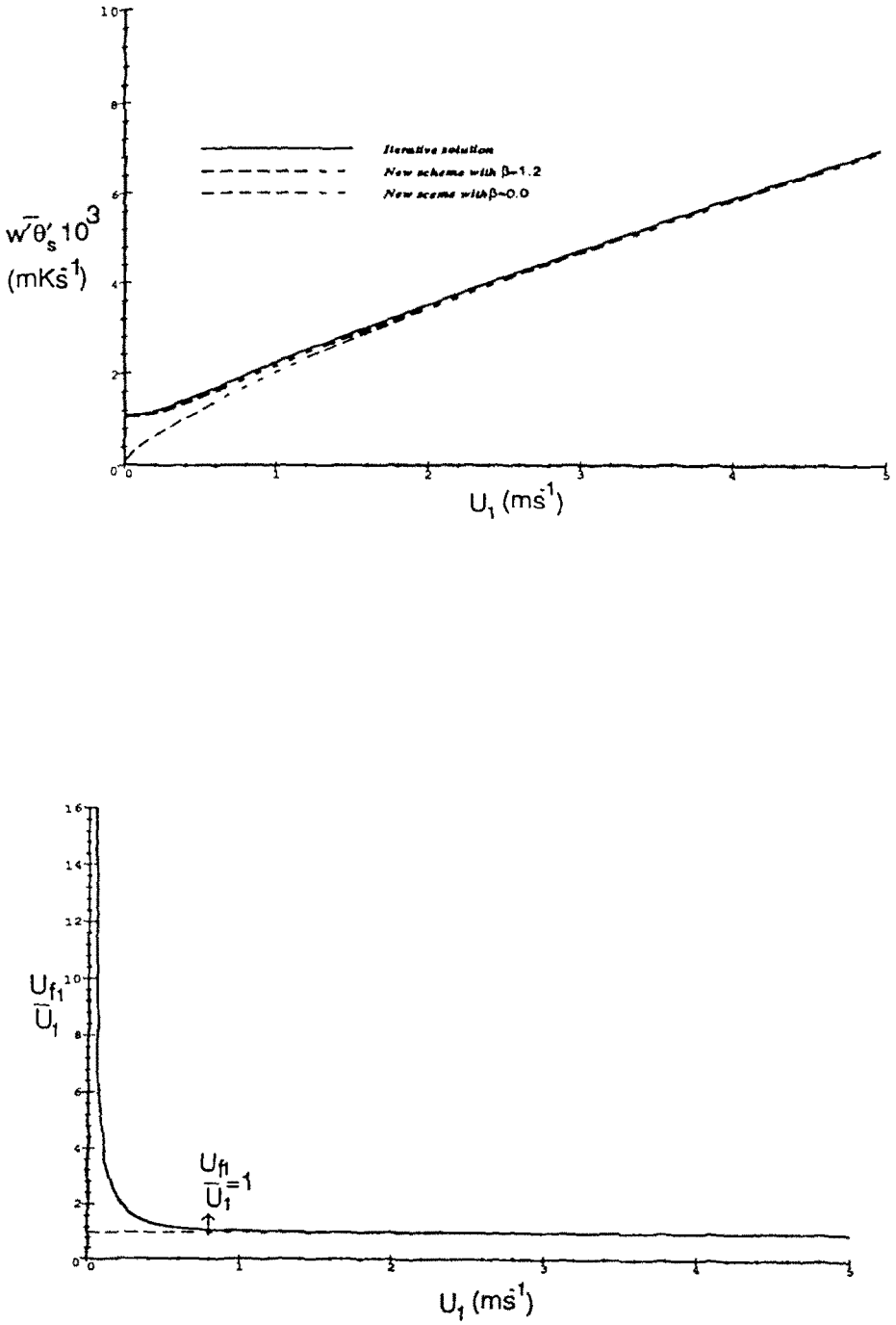

Figure 6. The same as in Figure 5 except with $z_1/z_0 = 7.5 \times 10^5$.

6. Results from GCM Simulations

To gain insight into the effect of changing the surface flux scheme alone, the new formulation was tested in the second generation model (GCMII). Apart from the formulation of surface fluxes this model is as described by McFarlane *et al.* (1992), except that climatological sea-surface temperatures and sea-ice cover were used instead of the static oceanic mixed layer and thermodynamic sea-ice model described in that paper.

The reference simulation (hereinafter designated as the CONTROL run) is comprised of ten successive annual cycles, each simulated with the standard model and the same (seasonally varying) climatological sea-surface temperature and sea ice cover fields. The simulation which uses the new surface flux scheme (hereinafter designated NEWFLUX) was carried out for three annual cycles, also using these climatological sea-surface temperature and sea-ice cover fields.

To maintain consistency with the old scheme, a lower limit (2 m s^{-1}) is imposed on the wind speed when it is used in computing surface heat and moisture fluxes in the NEWFLUX simulation. In this experiment we have not implemented the free convection formulation described in Section 4. We are presently testing a version of our scheme which has been modified to incorporate the free convection formulation. The lower limit on the wind speed is not imposed for that version. Results of this work will be reported at a later date.

The results presented below will, for the most part, be based on ensemble mean data for the December–February and June–August seasons. The choice of confining attention to these seasons is mainly for convenience. The features which we will discuss, though most clearly evident in the winter season, are found at all times of the year in various locations.

6.1. Effects on Surface Sensible Heat Flux and Air Temperature Fields

As discussed in Section 4 above, the new formulation tends to give larger upward heat flux values in unstable conditions for given values of lowest model level and surface prognostic variables. In stable conditions, however, the nature of the difference between the new and old schemes depends on location. Over land, the new scheme gives reduced downward flux values in stable conditions for all values of the bulk Richardson number. However, over water, fluxes determined using the old scheme vanish over open water for values of the bulk Richardson number exceeding the imposed threshold value (0.66). In these locations the new scheme gives enhanced downward fluxes in stable conditions.

These considerations are of importance in understanding the nature of the equilibrium response to the introduction of the new scheme in the numerical experiments. Over land surfaces and sea ice this response involves adjustments of both surface and lowest model level temperatures, while over open ocean surfaces only the lowest model level variables are allowed to respond.

In circumstances in which the surface layer is typically convectively unstable introduction of the new scheme would tend to reduce the degree of contrast between lowest model level and surface. This would be expected as well in typical convectively stable conditions over open oceans. However, over land and sea ice surfaces, the opposite effect is expected in typical stable conditions since the new scheme gives reduced downward heat fluxes for given values of the surface and lowest model level variables.

These effects are apparent in Figures 7a and b which show the ensemble mean differences between the NEWFLUX and CONTROL experiments for the surface sensible heat flux and lowest model level temperature fields respectively. The most pronounced differences in the temperature field are found in middle latitudes and polar regions over land and sea-ice surfaces in the winter hemispheres. In these regions the surface layer is generally stably stratified. Consequently, increases in lowest model level temperatures are associated with reduced downward heat flux (which appears as positive changes in the surface sensible heat flux since the sign convention used here is that upward fluxes are positive).

Surface temperature changes (not shown) in these regions are generally in the opposite sense to those at the lowest model level but much less pronounced. This field is sensitive as well to changes in snow cover and the associated changes in surface albedo.

Over oceanic regions adjacent to land and sea-ice surfaces in the high latitudes of the winter hemispheres negative regions in the sensible heat flux difference fields may represent enhanced downward fluxes rather than reduced upward fluxes. As discussed above, this response is associated with the fact that the new scheme gives generally larger downward fluxes in these regions when the surface layer is stably stratified. In these regions the stratification is typically transitional between the stable regime that is typically found over land and sea-ice surfaces in the winter and the near neutral or somewhat unstable conditions that are more typical over oceanic regions farther to the east and south. In those oceanic regions both heat flux and lowest model level temperature changes are generally smaller and consistent with the associated changes in upward sensible heat fluxes. For example, over the north-eastern Atlantic ocean in the winter season, cold air outbreaks can lead to stronger instability in these regions in winter, both in reality and in the model simulations. In these circumstances enhanced upward heat fluxes would be expected with the use of the new scheme. However, these are highly transient phenomena in which there is a rapid modification of the cold air masses. The ensemble mean state in these regions is more nearly neutrally stratified.

6.2. Effects on the Surface Energy Balance over the Oceans

On time scales longer than the local diurnal period there is a balance between sensible and latent heat fluxes and radiative fluxes over land surfaces. Such is not the case over the oceans of course (Boer, 1993). As illustrated in Figure 8 the

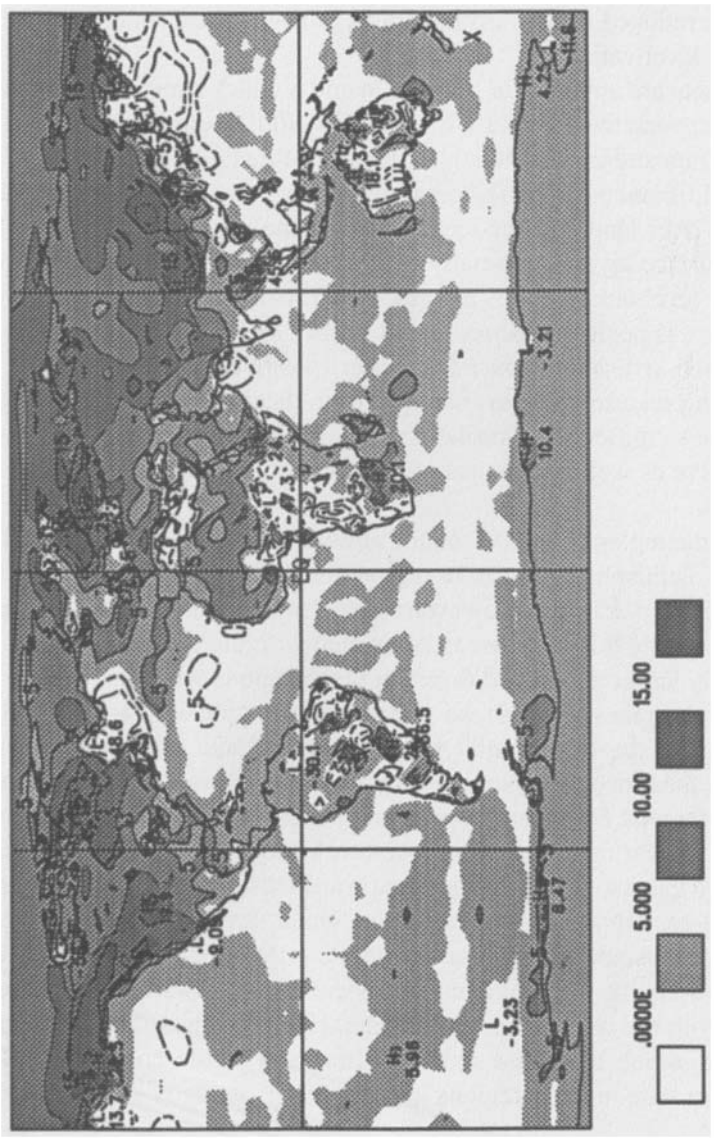

Figure 7a.

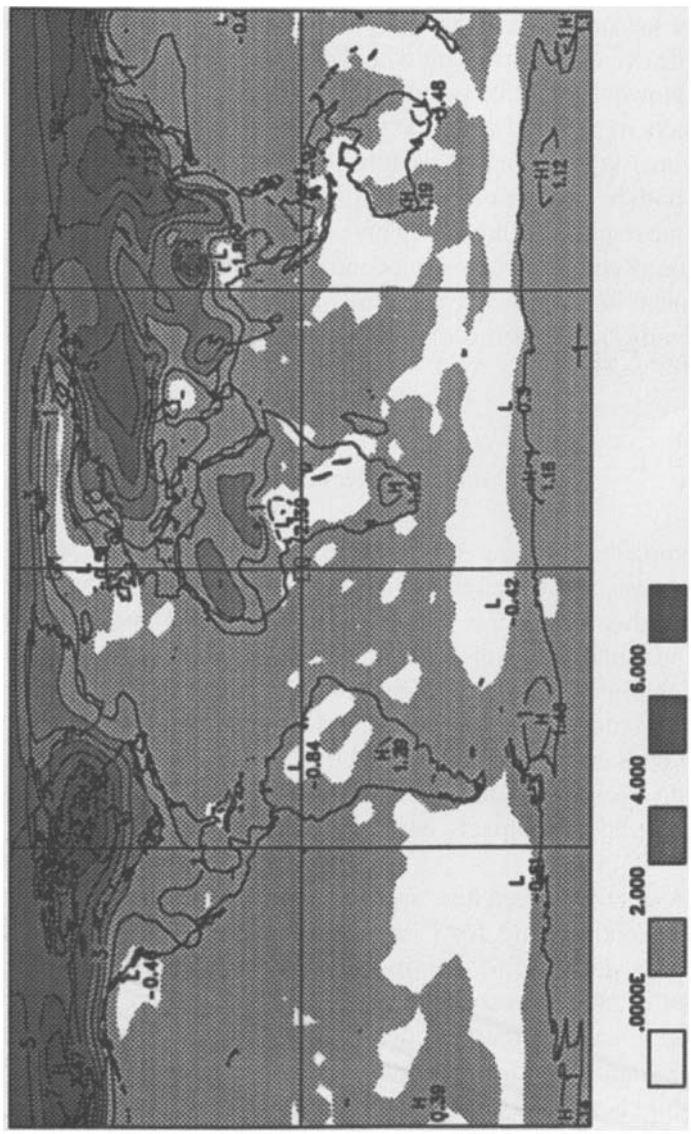

Figure 7. (a) Surface sensible heat flux, NEWFLUX-CONTROL with contour interval of 10 W m^{-2}. December–February. (b) Lowest level temperature, NEWFLUX-CONTROL with contour interval of 2 K. December–February.

oceans generally lose heat due to net upward fluxes in the winter hemisphere and gain heat in the summer hemisphere. A significant component of the surface energy flux in the tropics and sub tropics is the latent heat loss due to evaporation from the ocean surface.

The difference in the net surface flux is shown in Figure 9 for the northern hemisphere winter season. The increased net downward flux over the north western Atlantic and Pacific oceans is consistent with the changes in the surface heat fluxes in those regions. However positive values of the net flux changes in those regions represent the effects of reduced evaporative loss as well as reduced upward (or enhanced downward) sensible heat fluxes. In the North Atlantic ocean enhanced upward fluxes of both heat and moisture contribute to the negative values, while in the southern oceanic regions the broad negative regions are largely due to increased surface evaporation. Reduced evaporation contributes substantially to the positive values in the tropical and sub-tropical oceans, changes in both sensible and net radiative fluxes being both significantly smaller and/or more localized in those regions.

7. Concluding Remarks

The new parameterization for the surface fluxes presented in this paper avoids the computational costs associated with the fully iterative solution of the Monin–Obukhov similarity theory. The transfer coefficients obtained using the new parameterization are quantitatively consistent with the fully iterated solution. In contrast the transfer coefficients obtained using the GCMII and Louis's formulation are typically underestimated for unstable conditions over smooth surfaces and overestimated for both unstable and stable conditions over rough surfaces.

Results of multi-year simulation tests using GCMII show that the new parameterization has significant impacts on surface fluxes and the lowest level air temperatures.

Although the results presented here are from tests using the second generation AGCM of the Canadian Centre for Climate Modelling and Analysis, the new parameterization was designed for use in the third generation model (GCMIII). This third generation AGCM is still under development and, in its current form, differs in a number of ways from the operational GCMII. Apart from use of the new surface flux parameterization an additional difference is that the new model has substantially higher vertical resolution in the lower troposphere and the lowest model level is much closer to the surface. Additionally, some modifications to the formulation of heat and moisture transfer within the convectively active boundary layer have been incorporated.

The model also utilizes the CLASS land surface scheme (Verseghy *et al.*, 1993) in which surface roughness lengths for momentum, heat and moisture fluxes may differ from each other and vary with location as a function of surface soil and

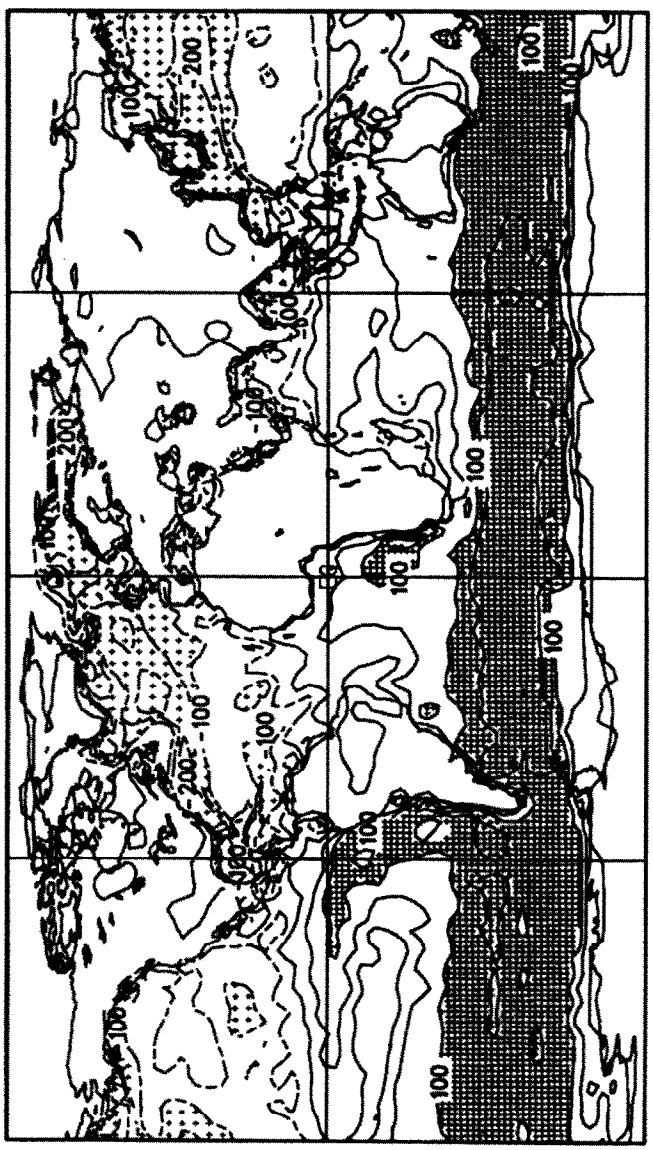

Figure 8. Net surface flux for the CONTROL with contour interval of 50 W m^{-2}. December–February.

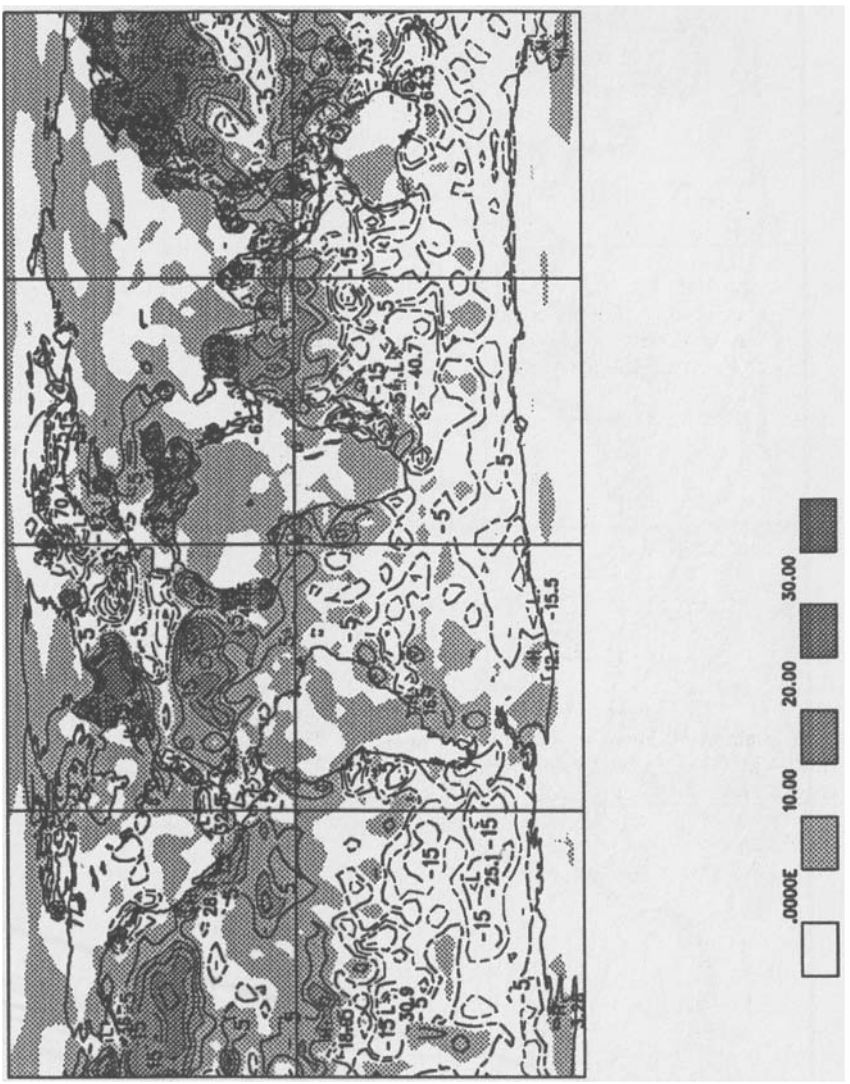

Figure 9. Net surface flux, NEWFLUX-CONTROL with contour interval of 10 W m^{-2}. December–February.

vegetation conditions. The new surface flux parameterization has been implemented in this land surface scheme for stand alone applications as well as for use in GCMIII.

Extensive multi-year simulations with GCMIII have not yet been completed. Tests using shorter simulations do indicate that the new surface flux parameterization has a significant and generally beneficial impact on the general performance of the model.

References

Beljaars, A. C. M.: 1995, 'The Parameterization of Surface Fluxes in Large-Scale Models under Free Convection', *Quart. J. Roy. Meteorol. Soc.* **121**, 255–270.

Beljaars, A. C. M. and Holtslag, A. A. M.: 1991, 'Flux Parameterization over Land Surfaces for Atmospheric Models', *J. Appl. Meteorol.* **30**, 327–341.

Boer, G. J., Arpe, J. K., Blackburn, M., Deque, M., Gates, W. L., Hart, T. L., Treut, H. Le., Roekner, E., Sheinin, D.A., Simmonds, I., Smith, R. N. B., Tokioka, T., Wetherland, R. T., and Williamson, D. L.: 1992, 'Some Results from an Intercomparison of the Climates Simulated by 14 Atmospheric General Circulation Models', *J. Geophys. Res.* **97**, 12771–12786.

Boer, G. J.: 1993, 'Climate Change and the Regulation of Surface Moisture and Energy Budgets', *Climate Dynamics* **8**, 225–239.

Businger, J. A., Wyngaard, J. C., Izumi, Y., and Bradley, E. F.: 1971, 'Flux Profile Relationship in the Atmospheric Surface Layer', *J. Atmos. Sci.* **28**, 181–189.

Carson, D. J. and Richards, P. J. R.: 1978, 'Modelling Surface Turbulent Fluxes in Stable Conditions', *Boundary-Layer Meteorol.* **14**, 67–81.

Dyer, A. J.: 1974, 'A Review of Flux-Profile Relationships', *Boundary-Layer Meteorol.* **20**, 35–49.

Garratt, J. R.: 1992, *The Atmospheric Boundary Layer*, Cambridge University Press, Cambridge, 316 pp.

Godfrey, J. S. and Beljaars, A. C. M.: 1991, 'On the Turbulent Fluxes of Buoyancy, Heat and Moisture at the Air-Sea Interface at Low Wind Speeds', *J. Geophys. Res.* **96**, 22043-2-48.

Hicks, B. B.: 1976, 'Wind Profile Relationships from the "Wangara" Experiment', *Quart. J. Roy. Meteorol. Soc.* **102**, 535–551.

Hogstrom, U.: 1988, 'Nondimensional Wind and Temperature Profiles in the Atmospheric Surface Layer: A Reevaluation', *Boundary-Layer Meteorol.* **42**, 55–78.

Holtslag, A. A. M.: 1984, 'Estimates of Diabatic Wind Speed Profiles from near Surface Weather Observations', *Boundary-Layer Meteorol.* **29**, 225–250.

Holtslag, A. A. M. and De Bruin, H. A. R.: 1988, 'Applied Modeling of the Nighttime Surface Energy Balance over Land', *J. Appl. Meteorol.* **27**, 689–704.

Large, W. G. and Pond, S.: 1982, 'Sensible and Latent Heat Flux Measurements over the Ocean', *J. Phys. Oceanogr.* **12**, 464–482.

Louis J. F.: 1979, 'A Parametric Model of Vertical Eddy Fluxes in the Atmosphere', *Boundary-Layer Meteorol.* **17**, 187–202.

McFarlane, N. A., Boer, G. J., Blanchet, J. P., and Lazar, M.: 1992, 'The Canadian Climate Centre Second-Generation General Circulation Model and its Equilibrium Climate', *J. Climate* **10**, 1013–1043.

Miller, M. J., Beljaars, A. C. M., and Palmer, T. N.: 1992, 'The Sensitivity of the ECMWF Model to the Parameterization of Evaporation from Tropical Oceans', *J. Climate* **5**, 1013–1043.

Monin, A. S. and Obukhov, A. M.: 1954, 'Basic Regularity in Turbulent Mixing in the Surface Layer of the Atmosphere', *Akad. Nauk. S.S.S.R. Trud. Geofiz. Inst.* **24**, 163–187.

Paulson, C. A.: 1970, 'The Mathematical Representation of Wind Speed and Temperature Profiles in the Unstable Atmospheric Surface Layer', *J. Appl. Meteorol.* **9**, 856–861.

Smith, S. D. and Banke, E. G.: 1975, 'Variation of the Sea Surface Drag Coefficient with Wind Speed', *Quart. J. Roy. Meteorol. Soc.* **101**, 665–673.

Townsend, A. A.: 1964, 'Natural Convection in Water over an Ice Surface', *Quart. J. Roy. Meteorol. Soc.* **90**, 248–259.

Uno, I., Cai, X. M., Steyn, D. G., and Emori, S.: 1995, 'A Simple Extension of the Louis Method for Rough Surface Layer Modelling', *Boundary-Layer Meteorol.* **76**, 395–409.

Van Ulden, A. P. and Holtslag, A. A. M.: 1985, 'Estimation of Atmospheric Boundary Layer Parameters for Diffusion Applications', *J. Climate. Appl. Meteorol.* **24**, 1196–1207.

Verseghy, D. L., McFarlane, N. A., and Lazar, M.: 1993, 'CLASS – A Canadian Land Surface Scheme for GCMs, II. Vegetation Model and Coupled Runs', *Int. J. Climatol.* **13**, 347–370.

Webb, E. K.: 1970, 'Profile Relationships: The Log-Linear Range and Extension to Strong Stability', *Quart. J. Roy. Meteorol. Soc.* **96**, 67–90.